

Theoretical and experimental investigation of magnetostrictive composite beams

Victor Giurgiutiu^{1,3}, Florin Jichi^{1,4,5}, Justin B Berman^{2,6} and Jason M Kamphaus^{2,7}

¹ Department of Mechanical Engineering, University of South Carolina, Columbia, SC 29208, USA

² US Army Corps of Engineers ERDC-CERL, Champaign, IL 61822-1076, USA

E-mail: victorg@sc.edu

Received 17 November 2000, in final form 18 July 2001

Published 3 October 2001

Online at stacks.iop.org/SMS/10/934

Abstract

Among novel non-destructive evaluation techniques for structural health monitoring, the magnetostrictive (MS)-tagged fiber-reinforced composites stands out as especially suitable due to: (a) distributed sensory properties, (b) non-contact damage detection, and (c) straightforward manufacturing implementation. Experimental data and mathematical modeling of a MS-tagged fiber reinforced composite beam under bending (flexural) loading are presented. A brief review of the state of the art identifies previous work on axially loaded MS composites, but finds no previous work on bending. Description of bending beam design and fabrication is followed by theoretical analysis and by the description of the experimental set-up and equipment used. Several analysis models were used. Test data, with and without applying magnetic bias field between loading cycles, is presented and results are discussed. Numerical values for the stress and strain versus magnetic flux density coefficients are given for both annealed and non-annealed cases. Piezomagnetic coefficients for the MS composite are calculated. The correlation between the results developed in the present paper for bending and previously published results for axial loading is found to be within 10% after correction factors depending on the quantity of the MS material.

(Some figures in this article are in colour only in the electronic version)

1. Introduction

In recent years, numerous civil engineering applications have started to use composite materials. This increase in composite materials usage raises the necessity for evaluating the in-service performance of such composite structures. The evaluation of a composite structure is a wide area in which engineers and researchers have proposed several in-service

non-destructive evaluation (NDE) technologies. Conventional NDE methods, initially developed for metallic structures, have been shown to be less effective in monitoring composites structures due to the micromechanical complexity of the composite material. New NDE technologies are required. The NDE technology analyzed in this paper is based on the inspectability of the advanced composite by using the magnetostrictive (MS) particle tagging technique. MS-tagged composites permit: (a) distributed sensory properties, (b) non-contact damage detection, and (c) straightforward manufacturing implementation.

³ Associate Professor.

⁴ Graduate Research Assistant.

⁵ Present address: Westinghouse Electric Company, Columbia, SC, USA.

⁶ Materials Engineer.

⁷ Graduate Research Assistant.

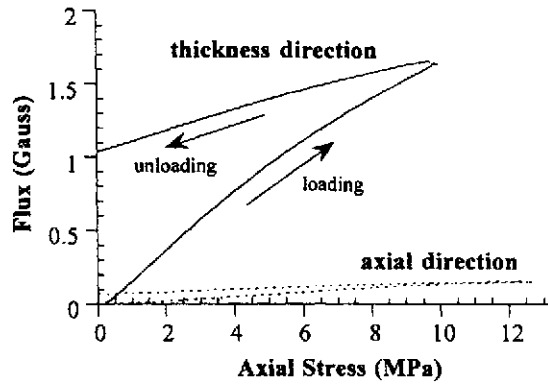


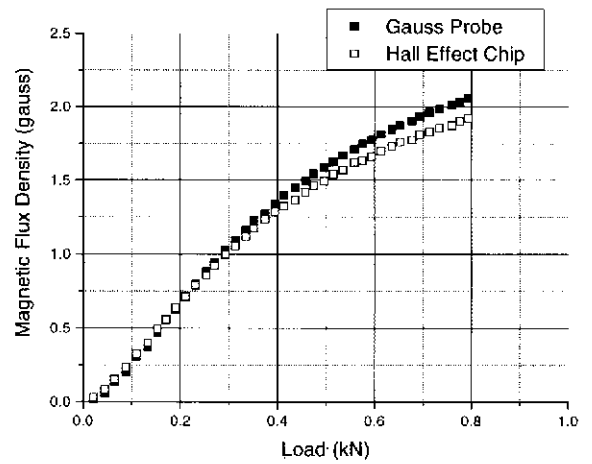
Figure 1. Magnetic flux in axial and thickness direction during axial loading of MS tagged composite beams (White 1999).

1.1. State of the art

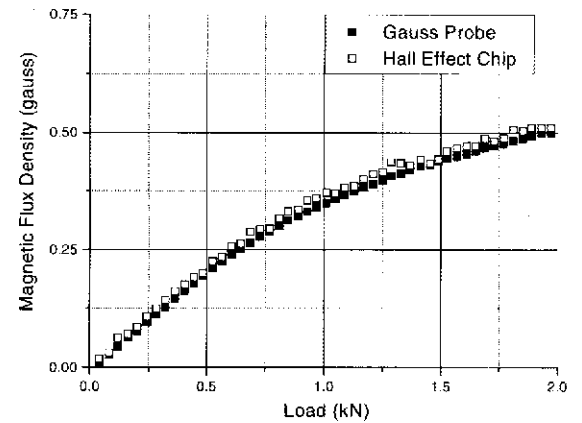
Terfenol-D is a magnetic anisotropy-compensated alloy $Tb_xDy_{1-x}Fe_2$ which shows a strong MS behavior. The name *Terfenol-D* represents the composition of the material and the original name of the Navy Laboratory at which the work began. *Ter* represents terbium, *Fe* from iron, *no*l Naval Ordnance Laboratory and *D* dysprosium. A MS material, such as Terfenol-D, subjected to mechanical strain produces a magnetic field. This phenomenon is known as the 'converse MS effect'. Research in MS-tagged composites for structural applications was started under the coordination of the US Army Construction Engineering Research Laboratory (Quattrone *et al* 1998). White and collaborators (White and Albers 1996, White *et al* 1996, White and Brouwers 1998, Hommema 1999) did extensive work on measuring the converse MS effect in MS-tagged composites under axial loading. White (1999) reviewed the MS tagging methodology of composites for structural health monitoring and gave an update on recent results. An experiment in which MS-tagged composite beams were subjected to uniaxial tension in a testing machine was presented. Neat resin beams tagged 2.24% by volume with MS Terfenol-D powder were used. The resulting magnetic field was measured in both the axial and thickness directions (figure 1). Trovillion *et al* (1999) studied the magnetic characteristics of neat resin and glass-fiber-reinforced MS composites subjected to axial load. The fiber-reinforced polymer composite (FRP) beams consisted of four layers of continuous strand glass mat fibers embedded in a polyester resin.

The top lamina of the composite was impregnated with Terfenol-D powder at a volume fraction of 2.24% for that lamina. The beams were subjected to uniaxial loading under load control at a rate of 0.02 kN s^{-1} . A gaussmeter probe and a small integrated-circuit Hall-effect device were used to measure the magnetic field response to subsequent loading and unloading. As seen in figure 2, both measuring devices gave similar results. Rearrangement of the magnetic dipole chains of the MS molecules through application of a strong magnetic field was performed by applying a magnetic field through the thickness of the beam using a pair of magnets to apply a field of 800 G.

Armstrong (2000) presented a new model of non-linear magneto-elastic behavior of MS particulate composites. The analysis assumed a uniform external magnetic field that is



(a)



(b)

Figure 2. Transverse magnetic flux density versus load: (a) neat resin and (b) composite sample (Trovillion *et al* 1999).

operating on a large number of well-distributed ellipsoidal MS particles encased in a elastic, nonmagnetic composite matrix. Nersessian and Carman (2000) studied five different volume-fraction particulate composites which were tested under two different conditions: (a) constant magnetic field and varying mechanical load and (b) constant mechanical load and varying magnetic field. Results for the constant magnetic field tests indicated that modulus increased with the volume fraction. Increase of modulus with the applied magnetic field value was also observed. The results presented for the constant load indicated a strong dependence of strain output on applied pre-stress.

Quattrone *et al* (1998) studied the magnetic response repeatability of MS tagged composites under cyclic loading. Terfenol-D active-tagged composites were subjected to uniaxial tension and the magnetic response in the axial direction under repeated loading and unloading was measured. Two types of experiments were performed: without applying a magnetic bias field between loading cycles (figure 3(a)) and with applying a magnetic bias field between cycles (figure 3(b)).

Krishnamurthy *et al* (1999) consider health-monitoring detection of delaminations in composite materials using an

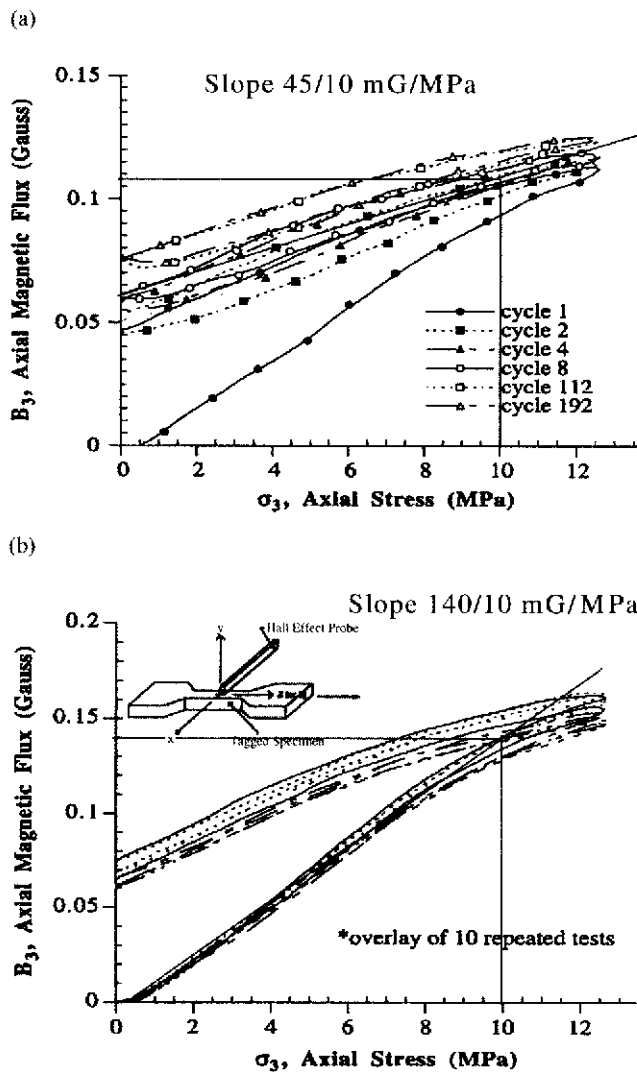


Figure 3. Stress/magnetic magnetic flux density for cyclic testing results: (a) without applying magnetic bias field between cycles and (b) with magnetic bias field applied between cycles (Quattrone et al 1998).

excitation coil and a sensing coil. The open-circuit voltage induced in the sensing coil is proportional to the stress generated in the MS layer by the presence of the delamination.

No previous experimental work on MS-tagged woven composites under bending could be found in the literature. In the present investigation, we performed studies of stress-strain and magnetic flux density response of a woven tagged composite subjected to a bending load. Several two-dimensional simulation models for strain and stress prediction in the composite were investigated. The analysis was performed under two separate assumptions regarding woven composites modeling: (a) balanced-orthotropic (BO) equivalent layers and (b) orthotropic cross-ply equivalent layers. The experimental investigation consisted of loading and unloading a simply supported MS-tagged composite beam using several centrally placed weights. The resulting strain and magnetic flux density were measured. Based on the experimental and analysis data, piezomagnetic stress and strain coefficients under bending loading were calculated. The piezomagnetic stress and strain coefficients determined in this paper for an MS-tagged composite under bending can be used

Table 1. Dimensions of the MS composite beam.

Characteristics	Dimension (mm)
Span (L)	600.0
Width (w)	100.0
Thickness (t)	6.50
Thickness of the lamina	0.929

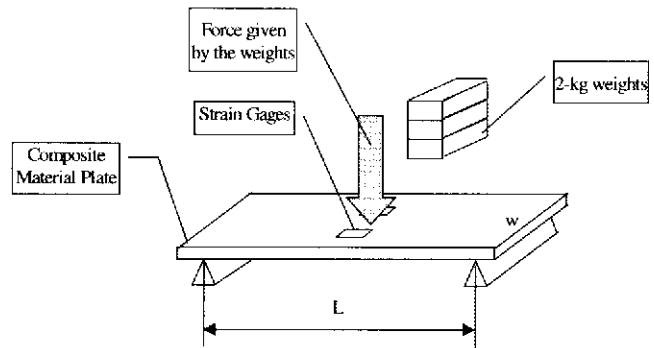


Figure 4. Schematic of the beam loading system.

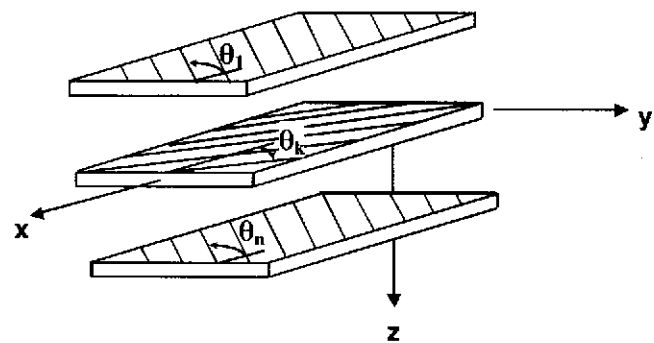


Figure 5. Schematic of a generic laminate.

in industry as reference data for the design of novel NDE devices based on MS-tagged composites.

2. Manufacturing of the magnetostrictive composite beam

An MS-tagged composite beam was fabricated by combining seven layers of a woven glass roving 36 oz/sq.yd. fabric and an Atlac 580-05 urethane-modified vinyl ester resin. The beam was 1000 mm long, and had a 100 mm by 6.5 mm cross section. MS Terfenol-D tagging powder was used in the two outer laminae in the middle 500 mm of the span. Of the 1000 g of resin used, 250 g had the MS powder. The resin was cured with 1% MEKP (methyl ethyl ketone peroxide) at room temperature for approximately 90 min. The target weight fraction of the glass fibers in the composite was $w_f = 30\%$. The weight fraction of MS Terfenol-D tagging was 15%. The dimensions of the beam are presented in table 1.

3. Analysis of magnetostrictive composite

The analytical work performed on the MS-tagged woven composite beam consisted of a micromechanical analysis and a lamination analysis. In the lamination analysis one BO and several cross-ply models were used. Convergence of the

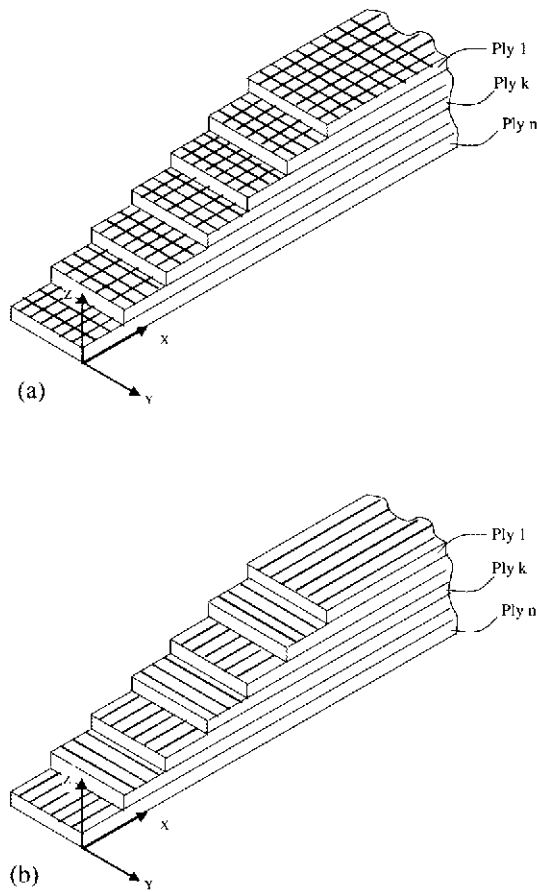


Figure 6. Comparison of the two lay-up models used in the analysis: (a) BO and (b) cross-ply.

predicted strain and stress values versus number of plies in the lamination model was also studied. A schematic of the loading system and how the load is applied to the beam is given in figure 4. The beam was simply supported at its ends, with 2 kg weights placed at its center.

3.1. Micromechanics analysis

Since a woven layer has fibers in two directions, warp and fill, the analysis of a woven composite layer cannot be directly performed using the classical lamination theory (CLT), which assumes lamina fibers are aligned in just one direction (Jones 1999). To translate woven fabric micromechanics properties for use with CLT, the equivalence principle needs to be applied. Tsai (1992) suggested that the predictions of elastic constants and strengths of woven composites could be made using classical micro- and macromechanics with appropriate empirical correction factors. One approach is to replace a woven composite layer with two equivalent conventional layers representing the fill and the warp of the original fabric. The micromechanics stiffness and strength formulae are then applied to the equivalent plies. One shortcoming of this approach is that the sequence order of the 0° and 90° plies may significantly affect the results.

Another approach is to replace the balanced woven composite layer by an orthotropic layer with averaged properties. For a woven composite having fibers aligned with the loading axes, this hypothesis yields BO behavior. In

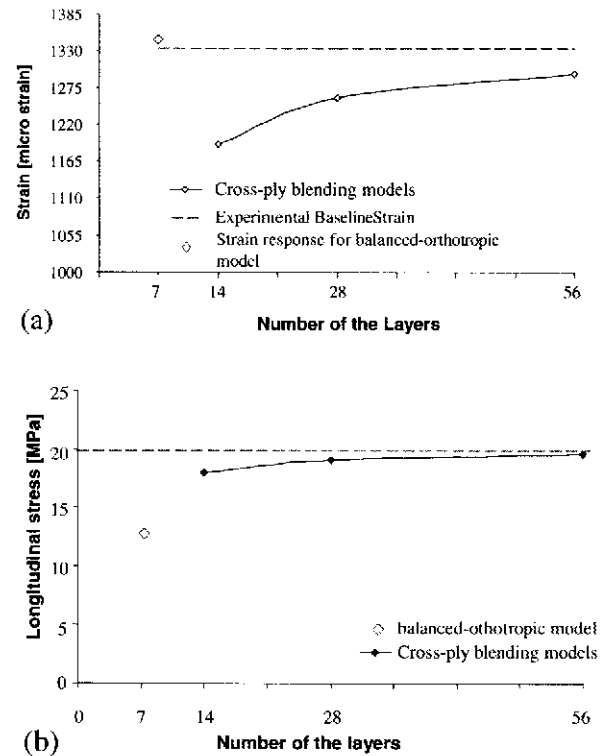


Figure 7. Convergence of results on the beam surface under maximum load condition ($F_{\max} = 58.9$ N, $M_{\max} = -88.29$ Nm m^{-1}) as predicted by various models and measured by experiment for: (a) strain results and (b) stress results.

our analysis, both approaches were taken. In either case, a conventional micromechanics analysis (Jones 1999) was first applied to determine the basic MS composite properties from the properties of its constituents (table 2).

The fiber volume fraction v_f is calculated as (Malik 1993, p 81, equation (2.5))

$$v_f = \frac{w_f}{\frac{w_f}{\rho_f} + \frac{1-w_f}{\rho_m}} \quad (1)$$

For the values given in table 2, the fiber volume fraction values yield $v_f = 0.16$.

Following Jones (1999), we calculated the basic moduli of elasticity in the material axes as

$$E_1 = E_L = E_f \cdot v_f + E_m \cdot v_m + E_{MS} \cdot v_{MS}$$

$$E_2 = E_T = [(E_f)^{-1} \cdot v_f + (E_m)^{-1} \cdot v_m + (E_{MS})^{-1} \cdot v_{MS}]^{-1} \quad (2)$$

The ply Poisson's ratio was calculated as

$$\nu_{12} = v_f \cdot \nu_f + v_m \cdot \nu_m + v_{MS} \cdot \nu_{MS} \quad (3)$$

Shear modulus for the fiber, matrix and Terfenol-D phases were defined as

$$G_f = \frac{E_f}{2 \cdot (1 + \nu_f)} \quad G_m = \frac{E_m}{2 \cdot (1 + \nu_m)} \quad (4)$$

$$G_{MS} = \frac{E_{MS}}{2 \cdot (1 + \nu_{MS})}$$

Table 2. Mechanical properties of the constituents of the MS woven composite beam.

Mechanical properties	Value
Young's modulus of the fiber, E_f^a	72.4 GPa
Young's modulus of the matrix, E_m^a	3.25 GPa
Young's modulus for the Terfenol-D, E_{MS}^b	30 GPa
Poisson ratio of the fiber, ν_f^a	0.2
Poisson ratio of the matrix, ν_m^a	0.3
Fiber density, ρ_f^d	2.54 g cc ^{-1c}
Matrix density, ρ_m^a	1.18 g cc ^{-1c}
Terfenol-D density, ρ_{MS}^c	9.25 g cc ^{-1c}
Thermal expansion coefficient for the fiber, α_f^a	5 × μm/m/°C
Thermal expansion coefficient for the matrix, α_m^a	3.0 am/m/°C
Thermal expansion coefficient for the Terfenol-D, α_{MS}^c	21.5 am/m/°C
Fiber weight fraction, w_f	30%
Terfenol-D powder (outer layers only)	
Average particle size	22.5 μm
Particle size range	1–45 μm
Volume fraction	2.24%

^a Malik (1993).
^b Butler (1988).
^c De Laicheisserie (1993).

In accordance with Jones (1999), the shear modulus for the plies was calculated as

$$G_{12} = \frac{G_f \cdot G_m \cdot G_{MS}}{\nu_f \cdot G_m \cdot G_{MS} + \nu_m \cdot G_f \cdot G_{MS} + \nu_{MS} \cdot G_f \cdot G_m} \quad (5)$$

The MS Terfenol-D volume fraction and Poisson's ratio were $\nu_{MS} = 2.24\%$ and $\nu_{MS} = 0.3$ for the plies with Terfenol-D, and zero for the other plies.

3.2. Lamination analysis

The elastic behavior of multidirectional plies can be described in terms of the stiffness matrix, the compliance matrix, and a set of engineering constants (Jones 1999). The goal is to determine the strain–stress distribution in the material. The plane-stress stiffness matrix $[Q]$ of an orthotropic composite ply is

$$[Q] = \begin{bmatrix} \frac{E_1}{1-\nu_{12}\nu_{21}} & \frac{\nu_{21}E_1}{1-\nu_{12}\nu_{21}} & 0 \\ \frac{\nu_{12}E_2}{1-\nu_{12}\nu_{21}} & \frac{E_2}{1-\nu_{12}\nu_{21}} & 0 \\ 0 & 0 & G_{12} \end{bmatrix} \quad (6)$$

where E_1 and E_2 are given by equation (2) and ν_{12} is given by (3). The composite is assumed to consist of a lay-up of multiple plies. The lay-up schematic for generic composite is presented in figure 5 where (x, y) coordinate axes are the loading axes.

Using the transformation matrix $[T]$, one computes the stiffness matrix in the loading axes:

$$[\bar{Q}] = [T]^{-1} \cdot [Q] \cdot [T]^{-1T} \quad (7)$$

Knowing the stiffness matrix of each ply, one calculates the $[A]$, $[B]$, and $[D]$ matrices for the composite laminate:

$$[A] = \sum_k [\bar{Q}]_{k-1} \cdot (z_k - z_{k-1}) \quad (8)$$

$$[B] = \frac{1}{2} \cdot \left[\sum_k [\bar{Q}]_{k-1} \cdot (z_k^2 - z_{k-1}^2) \right] \quad (9)$$

$$[D] = \frac{1}{3} \cdot \left[\sum_k [\bar{Q}]_{k-1} \cdot (z_k^3 - z_{k-1}^3) \right] \quad (10)$$

Hence, we write the general solution:

$$\begin{Bmatrix} \{\varepsilon^0\} \\ \{\kappa\} \end{Bmatrix} = \begin{bmatrix} [A] & [B] \\ [B] & [D] \end{bmatrix}^{-1} \cdot \begin{Bmatrix} \{N\} \\ \{M\} \end{Bmatrix} \quad (11)$$

where $\{N\}$ is the force vector, $\{M\}$ is the moment vector, $\{\varepsilon^0\}$ is the mid-surface strain vector, and $\{\kappa\}$ is the curvature vector. Using equation (9), the loading-axes strain at the top and the bottom of each ply is calculated as

$$\begin{aligned} \{\bar{\varepsilon}_{top_{k-1}}\} &= \{\varepsilon_0\} + z_{k-1} \cdot \{\kappa\} \\ \{\bar{\varepsilon}_{bot_{k-1}}\} &= \{\varepsilon_0\} + z_k \cdot \{\kappa\}. \end{aligned} \quad (12)$$

Using the loading-axes strains, the material-axes strains for the top and bottom of each ply are calculated:

$$\{\varepsilon\} = [T]^{-1T} \cdot \{\bar{\varepsilon}_{k-1}\}. \quad (13)$$

Consequently, the stresses in the longitudinal (L) and transversal (T) directions at the top and bottom of each ply are

$$\{\sigma_{top_{k-1}}\} = [Q]_{k-1} \cdot \{\bar{\varepsilon}_{top_{k-1}}\} \quad (14)$$

$$\{\sigma_{bottom_{k-1}}\} = [Q]_{k-1} \cdot \{\bar{\varepsilon}_{bot_{k-1}}\}. \quad (15)$$

The above analysis does not include thermal effects since the beam was cured and tested at room temperature.

3.3. Balanced-orthotropic and cross-ply models

The BO model, presented in figure 6(a), uses the assumption that a balanced woven composite can be represented by a composite having averaged properties. Using the longitudinal and transverse moduli of a uni-directional fiber composite layer, the averaged properties are given by

$$E_1 = E_2 = \frac{1}{2} \cdot (E_L + E_T). \quad (16)$$

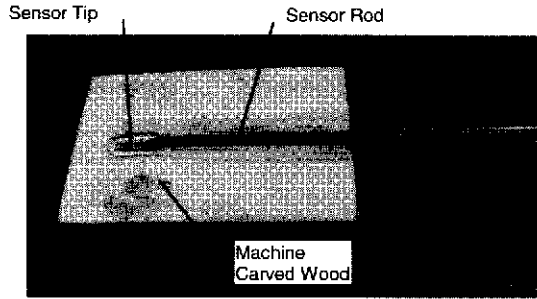


Figure 8. View of the assembly of magnetic sensor and protective carved wood fixture.

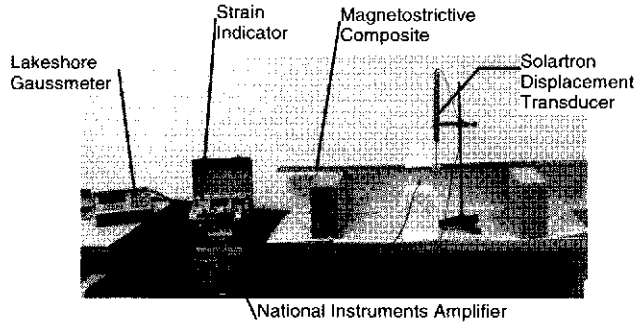


Figure 9. General view of the experimental set-up.

Performing the CLT analysis yields the BO matrices:

$$[A]_{BO} = \begin{bmatrix} 6.596 \times 10^7 & 7.291 \times 10^6 & 0 \\ 7.291 \times 10^6 & 6.596 \times 10^7 & 0 \\ 0 & 0 & 9.668 \times 10^6 \end{bmatrix} (\text{N m}^{-1}) \quad (17)$$

$$[B]_{BO} = \begin{bmatrix} 3.638 \times 10^{-12} & -2.274 \times 10^{-13} & 0 \\ -2.274 \times 10^{-13} & -9.09 \times 10^{-13} & 0 \\ 0 & 0 & 0 \end{bmatrix} (\text{N}) \quad (18)$$

$$[D]_{BO} = \begin{bmatrix} 244.47 & 25.897 & 0 \\ 25.897 & 190.99 & 0 \\ 0 & 0 & 34.346 \end{bmatrix} (\text{N m}). \quad (19)$$

In the cross-ply analysis (figure 6(b)), each woven composite layer is approximated by a couple of unidirectional cross-ply layers. The cross-ply layer can be either $0^\circ/90^\circ$ or $90^\circ/0^\circ$. Since the choice between $0^\circ/90^\circ$ and $90^\circ/0^\circ$ directly affects the accuracy of the results on the beam surfaces, we initially considered both cases in our analysis. It was found that $90^\circ/0^\circ$ produced small stresses at the specimen surfaces due to the transverse orientation of the fibers in the outer layers. Hence, the $90^\circ/0^\circ$ case was discarded, and the $0^\circ/90^\circ$ was retained for subsequent analysis. Additionally, the number of layers was gradually increased from 14 to 28 and 56, and a convergence study was performed. During this convergence study, as the number of layers was doubled, the thickness of the layer was correspondingly halved, such that the overall thickness of the beam was maintained. The 28- and 56-ply models were obtained by subsequent subdivision of the $0^\circ/90^\circ$ layers and application of symmetry principles. The ply angle distributions for the 14-, 28- and 56-ply models are presented in table 3.

Table 3. Lay-up of the composite models for the 14, 28 and 56 model.

Number of layers	Lay-up
14	$[(0/90)_3/0]_5$
28	$[(0/90)_7]_5$
56	$[(0/90)_{14}]_5$

The A , B and D matrices for the 56-ply model were

$$[A] = \begin{bmatrix} 6.22 \times 10^7 & 7.29 \times 10^6 & 0 \\ 7.29 \times 10^6 & 5.97 \times 10^7 & 0 \\ 0 & 0 & 9.67 \times 10^6 \end{bmatrix} (\text{N m}^{-1}) \quad (20)$$

$$[B] = \begin{bmatrix} -72.14 & -3.98 \times 10^{-13} & 0 \\ -3.98 \times 10^{-13} & 72.14 & 0 \\ 0 & 0 & 9.09 \times 10^{-13} \end{bmatrix} (\text{N}) \quad (21)$$

$$[D] = \begin{bmatrix} 224.47 & 25.90 & 0 \\ 25.90 & 211 & 0 \\ 0 & 0 & 34.35 \end{bmatrix} (\text{N m}) \quad (22)$$

3.4. Convergence analysis

The convergence of the strain and stress distribution for various models was studied. Attention was focused on the longitudinal stress and strain under maximum load conditions ($F_{\max} = 58.9 \text{ N}$, $M_{\max} = -8.83 \times 10^3 \text{ N m}$). The strain values predicted on the top and bottom surfaces were compared with the experimental value measured during the tests. The study shows that the largest strain value was predicted by the BO model. This value is also very close to the experimental value ($1347 \mu\epsilon$ versus $1333 \mu\epsilon$). The convergence of the strain distribution for the cross-ply models is apparent as the models becoming more refined, i.e. strain distribution is getting closer to the experimental data as the number of plies employed in the model is increased.

The predicted stress values are also shown in table 4. The stress distribution for the cross-ply models is substantially different from the stress distribution for the 7-ply BO model, i.e. the stresses predicted by the 14-, 28-, and 56-ply models are larger than the stresses predicted by the 7-ply BO model. Convergence of the strain and stress results in a graphical form is shown in figure 7. It can be appreciated that the BO model estimates strain well, but grossly underestimates the stress. The cross-ply models show definite convergence tendencies for both strains and stresses. It could be estimated that, by further increasing the number of layers in the model, convergence towards an asymptotic value of around 20 MPa would be obtained.

4. Experimentation of the magnetostrictive composite beam

The experimental results mentioned in table 4 of the previous section were obtained during a carefully conducted experiment. In this section, the equipment used in the experiment, the experimental set-up, the testing procedure, and the main results are presented.

Table 4. Comparison of the longitudinal strain and stress on the beam surface under maximum load condition ($F_{max} = 58.9$ N, $M_{max} = -8.83 \times 10^3$ N m) as predicted by various models and measured by experiment.

	7-ply BO model	14-ply 0°/90° model	28-ply 0°/90° model	56-ply 0°/90° model	Experiment
Strain ($\mu\epsilon$)	1347	1191	1259	1296	1333
Stress (MPa)	12.72	18.01	19.06	19.63	N/A

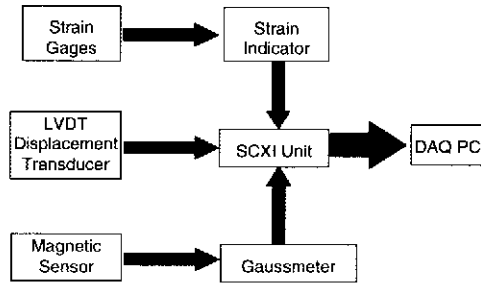


Figure 10. Schematic of the experiment and data flow.

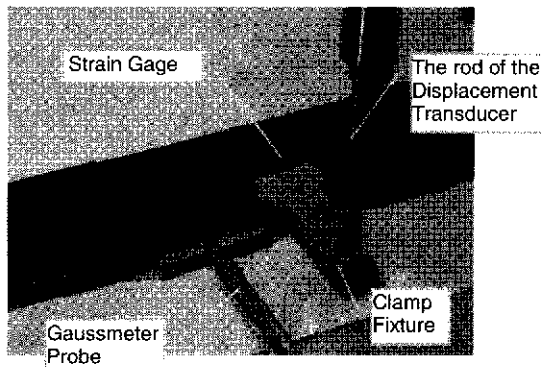


Figure 11. Position of the gaussmeter probe, strain gauge, and displacement transducer.

4.1. Experimental set-up

Many different pieces of equipment were used to achieve the simultaneous measurements of beam deflection, mechanical strains, and magnetic response of the MS-tagged composite. The equipment list is presented in table 5.

The beam was instrumented with strain gauges in the mid-span section on the upper and lower surfaces. The resulting magnetic flux density was measured with the gaussmeter. A special fixture had to be constructed to ensure consistent alignment of the gaussmeter probe with the composite surface and to mechanically protect it. The tip of the gaussmeter probe is made of ceramic and covers the magnetic sensor. Considering how fragile the gaussmeter probe is and on the advice from Lakeshore Cryotronics, the protective wood fixture shown in figure 8 was designed and fabricated. The distance from the tip of the sensor to the upper surface of the beam was 2 mm. The open area was covered with clear tape. The sensor rod was attached to the wood fixture using Pro Seal Blue RTV Silicone made by Pacer Technology (Rancho Cucamonga, CA). The overall configuration of the experiment is shown in figure 9.

Data flow of the simultaneously measured beam deflection, mechanical strains, and magnetic response of the MS-tagged composite beam through the data acquisition and

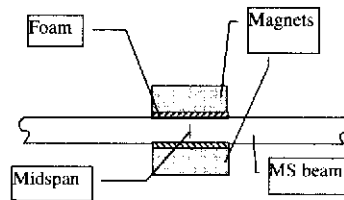


Figure 12. Schematic of the position of the magnets during magnetic bias field application.

processing modules is presented schematically in figure 10. The strain gauges placed on both the upper and lower surfaces of the beam at the mid-span position were connected in a half bridge configuration to the strain indicator. The magnetic flux density produced by the MS particles was measured by the gaussmeter.

For correlation purposes, the mid-span displacement was also measured. An LVDT displacement transducer and a non-magnetic (aluminum and brass) clamping fixture were used. Details of the mid-span instrumentation showing the strain gauges, displacement transducer, and gaussmeter probe are given in figure 11. Initial trials showed that the strain gauge and LVDT electromagnetic fields did not influence the gaussmeter reading of the induced magnetic field.

4.2. Testing procedure for MS composite beam bending experiment

The MS-tagged composite beam, supported on concrete blocks (500 mm equivalent span), was loaded gradually with 2 kg weights. In order to avoid excessive strain in the composite material, the number of loading weights was limited to three. The test procedure was as follows: gradually load the beam, acquire data and repeat until all the weights were on the beam. Next, reverse the procedure under gradual unloading. The strain gauges were connected to a strain indicator, which provided the actual strain value at the top and bottom surfaces. At the same time, the displacements were measured with an LVDT. Hence, the relationship between loads, displacements and strains could be established. Simultaneously, the magnetic field developed by the MS active tagging particles was detected using the gaussmeter. The gaussmeter provided the value of the magnetic flux density read by the probe on the surface of the MS-tagged composite material. The data was collected using National Instruments LabView software and associated hardware consisting of a SCXI signal-conditioning module, and a Gateway computer. The information was processed using National Instruments LabView software. The data collection was developed for simultaneous on-line operation with the strain gauges, displacement transducer and the gaussmeter. At each loading step, complete data collection was performed.

Table 5. List of the equipment used in the MS composite beam experiment.

Name	Model	Manufacturer
Strain gauges	CEA-06-125UT-120	Measurement Group, Inc.
Strain indicator	P-3500	Measurement Group, Inc.
Gaussmeter	Model 450	Lakeshore Cryotronics, Inc.
LVDT displacement transducer	B-50	Solartron Company
SCXI amplifier unit	SCXI-1000	National Instruments Company
Lab View	NI Professional Measurement Suite	National Instruments Company
PCMCIA card	DAQcard-AI-16E-4 16 channel	National Instruments Company
Composite material		Reichhold Chemicals
Permanent magnets	6" × 4" × 1" Ceramic 8 Magnet	Adams Magnetic Products
Gateway computer	G6-200	Gateway Inc.

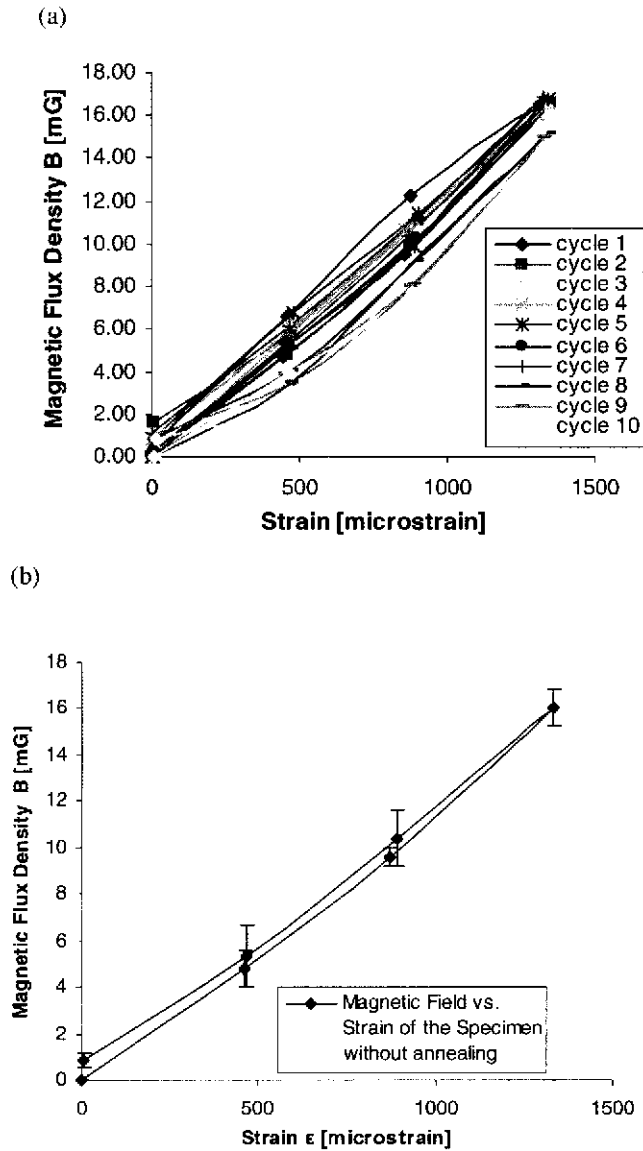


Figure 13. Magnetic flux density response to bending strain measured on the bottom surface of MS-tagged composite beams: (a) superposed 10 consecutive cycles and (b) mean values of magnetic flux density and standard deviation versus strain for the beam. Note: no magnetic bias field was applied between cycles.

4.3. Applying magnetic bias field between cycles

In some of the experiments, a strong magnetic field that aligns the magnetic moment of each individual domain of the MS-tagging particles was applied between loading cycles. Thus,

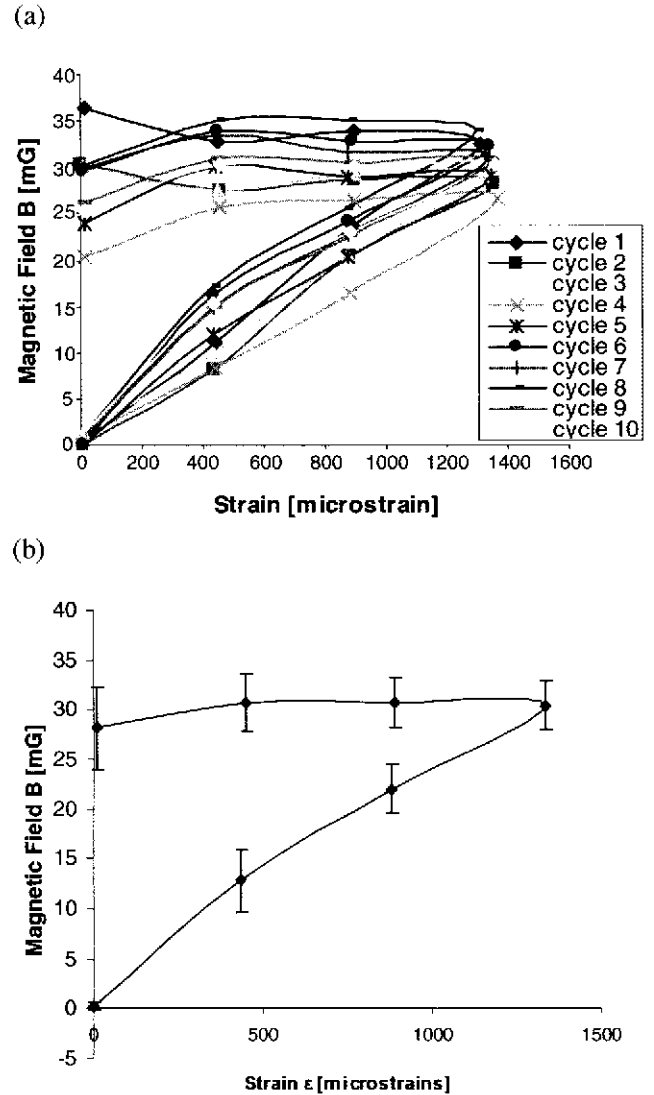


Figure 14. Experimental magnetic flux density results versus strain cycles measured on the bottom surface of MS-tagged composite beams: (a) ten cycles superposition and (b) mean and standard deviation. Note: a magnetic bias field was applied between cycles.

the initial response under load was enhanced. We used a pair of permanent magnets (Adams Magnetic Products, Garland, TX) generating a magnetic flux density of 740 G. The magnetic bias field was applied with the beam in the no-load position. The application of the bias magnetic field between cycles took, on average, 1.5 min. The positioning of the magnets is presented in figure 12.

4.4. Results for the experiments without applying a bias magnetic field between cycles

First, experiments were conducted without applying a bias magnetic field between cycles. When these experiments were performed and the data was acquired, the beam had not been subjected to a bias magnetic field for more than two days. Thus, the results are indicative of the response of a field-deployed MS-tagged composite material. Ten loading–unloading cycles were performed of the strain and displacement data. Linearity and repeatability versus the force data was observed. The strain hysteresis was less than 2%. This is acceptable and falls within the accuracy of the data acquisition card and National Instruments amplifier.

The magnetic flux density response of the beam is presented in table 6. The zero load reading was subtracted from the other values in order to eliminate the influence of the environmental magnetic field. The ten cycles considered in the experiment show the reproducibility of the magnetic flux results.

It was noticed that some difference in magnetic flux density readings resulted between cycles, though the strain and displacement readings were almost identical. This difference between cycles in magnetic flux density readings could be due to hysteresis in the MS material. It could also reflect experimental error, since the magnitude of the stress-induced magnetic flux density is rather small, of the order of milligauss, and hence fluctuations in the environmental magnetism may impact these readings.

The relationship between magnetic flux density and strain is presented in figure 13. Figure 13(a) shows the raw data of magnetic flux density versus strain obtained during the ten cycles. It can be seen that the relationship between strain and magnetic flux density is consistent and repeatable. One can also see that the magnetic flux has a small hysteresis. This phenomenon is present because of changes in the microscopic magnetic status of the tagging particles (White and Brouwers 1998). The small difference between readings in different cycles illustrates the deviation expected from the use of general-purpose magnetic flux density measurement equipment. Figure 13(b) presents the mean values of the experimental results. These observations indicate that non-annealed MS-tagged composites in bending present satisfactory repeatability and small hysteresis. White and Brouwers (1998) made similar observations for axially loaded beams and axially measured magnetic fields.

4.5. Results with a bias magnetic applied between loading cycles

In these experiments, a bias magnetic field was applied between loading cycles. Again, ten loading–unloading cycles were conducted. Displacement, strain and magnetic field levels were collected and analyzed. The strain and displacement results showed a very good repeatability with less than 1.7% standard deviation. The experimental magnetic field data are given in table 7. The 10 cycles show that the measurements are repeatable and consistent. As in the experiment conducted without applying a bias magnetic field between cycles, the small difference between readings in different cycles illustrates the deviation to be expected from

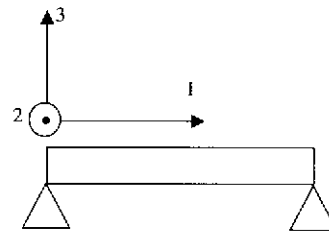


Figure 15. Schematic of the coordinate system used in magnetic flux measurements.

the use of general-purpose magnetic flux density measurement equipment.

The plot of magnetic flux density versus strain is given in figure 14. It can be seen that, on the increasing branch of the curve, the magnetic field response is almost linear. The maximum magnetic flux values are about double the values obtained without applying a bias magnetic field between cycles (32 mG versus 16 mG, respectively). This proves that applying a bias magnetic field between cycles increases the initial MS response. The increasing branch also shows a slight negative curvature, i.e. the marginal response per unit load becomes less pronounced as the load increases. On the decreasing branch of the curve, significant hysteresis is present and the marginal response is very small. These observations indicate that MS-tagged composites possess a higher initial response, but also a very pronounced hysteresis. Mean average and standard deviation of the magnetic flux density calculated using statistical methods are plotted in figure 14(b).

5. Effective piezomagnetic coefficients of the magnetostrictive composite

For monolithic MS Terfenol-D material, the piezomagnetic coefficients, e_{31} , and d_{31} are well known and available from standard references (Butler 1988, De Lacheisserie 1993). These coefficients correlate the magnetic flux density, B_3 , with the strain, ϵ_1 , and stress, σ_1 . The directions of the stress and magnetic flux density are using the coordinate system presented in figure 15.

For MS-tagged composites, such simple relationships cannot be directly established, since the composite contains three separate phases (fiber, resin, and MS-tagging powder) of which only one is MS. However, effective piezomagnetic coefficients can be established to allow a macroscale relationship between the recorded magnetic flux density and the strain and stress in the tagged composite. To this purpose, we have calculated both the e_{31} and the d_{31} coefficients, as shown in the following sections. The e_{31} coefficient was calculated because it can be determined directly from the measured strain and magnetic flux. The d_{31} coefficient was calculated in order to facilitate comparison with the d_{31} data reported in the literature for axially loaded MS composite beams. It should be noted that the d_{31} coefficient cannot be determined directly from experimental data alone, since no simple device exist to directly measure the stress inside an composite beam in bending. We determined the d_{31} coefficient using the stress predicted by the lamination analysis, and the magnetic flux density measured during the experiments.

Table 6. Magnetic flux density results for the not-annealed beam.

Force F (N)	Magnetic flux density, B (mG)										Average value	Standard deviation %
	Cycle 1	Cycle 2	Cycle 3	Cycle 4	Cycle 5	Cycle 6	Cycle 7	Cycle 8	Cycle 9	Cycle 10		
0	0.00	0.00	0.00	0.00	0.00	0.00	0.00	0.00	0.00	0.00	0	0
19.62	4.73	4.79	5.67	5.57	5.39	5.25	5.41	3.36	3.88	3.92	4.79	0.16
39.24	9.48	9.96	10.68	10.64	9.92	10.39	8.96	8.96	7.98	7.73	9.56	3.97
58.86	16.60	16.53	16.63	16.05	16.74	16.37	16.85	15.15	15.02	14.43	16.03	5.05
39.24	12.27	11.08	10.96	10.65	11.41	10.23	11.11	9.26	8.15	8.86	10.39	11.54
19.62	6.62	5.85	6.31	5.94	6.79	5.3	6.14	4.07	3.49	2.69	5.31	25.23
0	0.87	1.6	0.62	0.81	0.58	0.29	1.09	0.81	1.06	0.89	0.86	38.37

Table 7. Experimental magnetic flux density results for the annealed beam.

Force F (N)	Magnetic flux density B (mG)										Average value	Standard deviation %
	Cycle 1	Cycle 2	Cycle 3	Cycle 4	Cycle 5	Cycle 6	Cycle 7	Cycle 8	Cycle 9	Cycle 10		
0	0.05	0.00	1.6	0.70	-0.25	-0.05	-0.05	0.47	0.33	0.64	0.3	0
19.62	11.03	8.18	9.98	8.42	11.92	16.18	14.99	17.10	14.88	15.29	12.80	24.37
39.24	23.88	20.63	50.45	16.45	20.43	24.14	22.89	25.5	22.64	23.02	21.99	11.09
58.86	32.59	28.19	29.18	26.75	29.05	32.5	31.23	33.91	30.65	30.37	31.43	7.85
39.24	33.79	28.69	29.38	26.37	28.81	32.93	31.54	34.94	30.56	30.13	30.71	8.04
19.62	32.84	27.57	27.63	25.83	30.02	33.88	33.42	35.11	30.87	30.36	30.75	9.46
0	36.34	30.27	29.95	20.33	24.03	29.49	29.72	30.06	26.20	25.29	28.17	14.73

Table 8. Summary of MS coefficients for MS-tagged composites, as determined in this paper and by previous investigators (see Note).

Characteristic	Bending load (present investigation)		Axial load (Quattrone <i>et al</i> 1996)	
		With magnetic field bias between cycles		With magnetic field bias between cycles
Composite type	Woven	Woven	Neat resin	Neat resin
Chained	No	No	Yes	Yes
Measured B field direction	Transverse	Transverse	Axial	Axial
Piezomagnetic stress coefficient (N Am^{-1})	$e_{31} = 13.7 \times 10^{-4}$	$e_{31} = 24.5 \times 10^{-4}$	X	X
Piezomagnetic strain coefficient (m A^{-1})	Raw data Compensated for MS volume fraction	$d_{31} = 10.2 \times 10^{-14}$ $d_{31} = 33.7 \times 10^{-14}$	$d_{31} = 15.6 \times 10^{-14}$ $d_{31} = 51.5 \times 10^{-14}$	$d_{31} = 40 \times 10^{-14}$ $d_{31} = 140 \times 10^{-14}$

Note: The tensile data were published by Quattrone *et al* (1998). The bending results were obtained in the present investigation and were first published by Giurgiutiu *et al* (1999a, 1999b). The piezomagnetic coefficients were calculated by the authors of the present paper from the data published in the references cited above.

5.1. Piezomagnetic coefficients

According to De Lacheisserie (1993), the piezomagnetic stress coefficient, e_{31} , defines the relationship between the applied strain, ε_1 , and the resulting flux density, B_3 , in the form

$$B_3 = e_{31} \cdot \varepsilon_1. \quad (23)$$

We calculated the piezomagnetic stress coefficient, e_{31} , using the plot of the average values of the experimentally determined B_3 - ε_1 curves. The determined e_{31} values were entered in table 8.

Likewise, according to De Lacheisserie (1993), the piezomagnetic stress coefficient, d_{31} , defines the relationship between the applied strain, σ_1 , and the resulting flux density, B_3 , in the form

$$B_3 = d_{31} \cdot \sigma_1. \quad (24)$$

We calculated the piezomagnetic stress coefficient, d_{31} , using the plot of the average values of the experimentally determined magnetic flux density, B_3 , and the calculated stress, σ_1 . The use of calculated stress in this determination needs a little explanation. No experimental device exists for directly measuring stress. In our investigation, we used several lamination models (7-ply through 56-ply), and compared their predicted stress with experimentally measured values (table 3). This showed that the 56-ply model was the most adequate. Consequently, we used the stress predicted by the 56-ply model in the determination of the d_{31} coefficient.

5.2. Comparison with other investigators

The present authors used the experimentally derived curves reported by other investigators (Quattrone *et al* 1998) to identify average values of stress-magnetic flux density

coefficients (figure 3). These coefficients express the magnetic flux density developed when a given axial stress is applied to the MS-tagged neat resin composite beam (please recall that the piezomagnetic stress coefficient defines magnetic flux density per unit strain, and vice versa). The values of these coefficients were entered in the last two columns of table 8.

Table 8 shows that the raw piezomagnetic strain coefficients obtained in our composite experiments seems to be about 4–10 times lower than those published by Quattrone *et al* (1998) for neat resin tension beams. The reasons for this difference are:

- (1) The stress distribution was different, i.e. bending versus axial. The axial stress distribution is uniform in the cross section, while the bending distribution is linearly varying from maximum positive to negative values. Hence, only a small portion of the composite (outer fibers) is actually loaded to the maximum stress. Thus, for the same stress values in the outer fibers, a tensile beam will produce much more magnetism than a bending beam. Since the gaussmeter probe was measuring the overall response, it results that its readings are expected to be lower in the bending beam than in the tensile beam.
- (2) Quattrone *et al* (1998), by performing tensile experiments, measured the magnetic flux density, B_3 , parallel to the applied stress, σ_3 . In our bending experiments, the applied load generated stress in the σ_1 , which is perpendicular to the direction of the measured B_3 .
- (3) In the tensile neat-resin beams used by the previous investigators, the Terfenol-D particles were dispersed throughout the neat resin body, whereas in our composite bending experiments an important portion of the beam was occupied by the reinforcing fibers. Hence, the Terfenol-D particles could only be dispersed in the 81% volume allocated to resin. Additionally, Terfenol-rich resin was applied only in the outer layers of the composite lay-up. In essence, this means that, in our composite bending beams, the Terfenol volume ratio was 0.68%, whereas in neat resin tensile beams it was 2.24%, which is 3.3 times higher.

When the difference in MS-tagging volume fraction was compensated for, the values of piezomagnetic strain coefficients measured by us in bending without bias magnetic field applied between cycles became comparable with those measured by Quattrone *et al* (1998) under axial loading and similar conditions. This shows convergence of the two investigations and increased confidence in the industrial application potential of this technology.

6. Conclusions

This paper has presented theoretical and experimental data resulting from the study of a MS-tagged fiber-reinforced composite beam under bending. A brief review of the state of the art revealed that there has been no previously published work on the magnetic response of a MS-tagged composite under a bending load, which emphasizes the importance of this investigation for the advancement of the state of the art in this field. A MS-tagged composite bending beam was designed, fabricated, and tested. An analysis procedure of laminate woven composites was applied to predict the state of stress and

strain in a simple supported composite beam. Convergence of results was studied using an increasing number of layers from 7 to 56. The main equipment, experimental set-up and testing procedure have been described. Test data was obtained with and without applying a bias magnetic field between loading cycles. The results were processed and presented in terms of magnetic response versus measured strain and versus predicted stress. For tests without applying a bias magnetic field between cycles, the results showed linearity and low hysteresis. For tests with applying a bias magnetic field between cycles, an increase in initial response and a very pronounced hysteresis were both observed.

The piezomagnetic stress coefficient, e_{31} , was calculated using measured magnetic flux versus measured strain. The piezomagnetic strain coefficient, d_{31} , was also calculated using the measured magnetic flux density and the stress predicted by a 56-ply model with 0/90 cross-ply layers. Comparison between the present bending results and the previously published results for axial loading was performed.

This investigation has shown that a clear relationship can be established between the magnetic flux density measured at the surface of a MS-tagged composite and the stress state inside the beam. Previous investigators had proved this relationship for axial loading. In this paper, for the first time, MS-tagged composite results under bending loading are presented. Both axial results (presented by previous investigators) and bending results (presented in this paper) indicate a good consistency and repeatability of the magnetic flux response resulting from loading and unloading of the MS-tagged composite.

The impact of using MS-tagged composites for in-service NDE of composite structures could be very significant. Unlike conventional strain measuring methods that use strain gauges, which are permanently applied on the structure and wired to the measuring equipment, the MS-tagging method can be used by simple surface scanning using a traveling magnetic flux gauge. This opens up the opportunity for measuring stress patterns in large structures in order to identify stress distributions and 'hot spots'.

At present, the MS-tagging NDE methodology is still in its infancy. Considerable work needs to be done before large-scale industrial implementation is possible. Further research work needs to cover: (a) development of portable, hand-held equipment for magnetic flux measurement of large structural areas using surface scanning techniques, (b) further characterization of the magnetic response of MS-tagged composites of various tagging densities and distributions, and (c) evaluation of long-term behavior under various environmental conditions. The piezomagnetic stress and strain coefficients determined in this paper for MS-tagged composites under bending can be used in industry as reference data for the design of novel NDE devices based on the MS effect in MS-tagged composites.

Acknowledgments

The authors acknowledge the financial support of US Army Corps of Engineers Construction Engineering Research Laboratory (CERL) through contract no DACA88-98-K-0001. The support of the Market Development Alliance and especially Reichhold Chemicals Inc. is also gratefully acknowledged.

References

- Armstrong W D 2000 A general magneto-elastic model of Terfenol-D particle actuated composite material *Adaptive Structures and Materials 2000, ASME Int. Mechanical Engineering Congress and Exposition (Orlando, FL, Nov. 2000)* (Fairfield, NJ: ASME International) pp 127–37
- Butler J L 1988 Application manual for the design of Etrema terfenol-d magnetostrictive transducers *Etrema Products Inc.* 1–10
- De Lacheisserie E du T 1993 *Magnetostriction-Theory and Applications of Magnetoelasticity* (Boca Raton, FL: CRC Press) pp 53–6
- De Lacheisserie E du T 1993 *Magnetostriction-Theory and Applications of Magnetoelasticity* (Boca Raton, FL: CRC Press) 345–7
- Giurgiutiu V, Jichi F, Rogers C A, Quattrone R and Berman J B 1999a Experimental study of magnetostrictive tagged composite strain sensing response for structure health monitoring *2nd Int. Workshop of Structural Health Monitoring (Stanford University, Sept. 1999)* (Lancaster, PA: Technomic) pp 690–9
- Giurgiutiu V, Jichi F and Rogers C A 1999b Design, fabrication and testing of a magnetostrictive-tagged fiber-reinforced composite beam *Report USC-ME-LAMSS-99-106*
- Hommema J A 1999 Magnetomechanical behavior of terfenol-d particulate composites *Master's Thesis* Department of Theoretical and Applied Mechanics, University of Illinois (Urbana-Champaign)
- Jones R M 1999 *Mechanics of Composite Materials* (New York: Hemisphere)
- Krishnamurthy A V, Anjanappa M, Wang Z and Chen Z 1999 Sensing of delaminations in composite laminates using embedded magnetostrictive particle layers *J. Intell. Mater. Syst. Struct.* **10** 825–35
- Malik P K 1993 *Fiber-Reinforced Composites. Materials, Manufacturing and Design* 2nd edn (New York: Marcel Dekker)
- Nersessian N and Carman G 2000 Magneto-mechanical characterization of magnetostrictive composite *Adaptive Structures and Materials 2000, ASME Int. Mechanical Engineering Congress and Exposition (Orlando, FL, Nov. 2000)* pp 139–45
- Quattrone R F, Berman J B, Chaudhry Z, Giurgiutiu V, Rogers C A and White S R 1998 *Investigation of Active Tagged Composites for Army Infrastructure Applications* CERL TR 98/022, ADA344919 (Springfield, VA: NTIS)
- Quattrone R, Berman J B and White S R 1998 Self-monitoring structures containing magnetostrictive composite *Proc. 21st Army Science Conf. (Norfolk, VA, June 1998)* (Springfield, VA: NTIS) pp 21–6
- Trovilleion J, Kamphaus J, Quattrone R and Berman J 1999 Structural integrity monitoring using smart magnetostrictive composites *Proc. Int. Composites EXPO'99 (Cincinnati, OH, 1999)* Session 22-D (New York: Composites Institute) pp 1–6
- Tsai S 1992 *Theory of Composites Design* (Dayton: Think Composites)
- White S R and Albers R G 1996 Magnetostrictive tagging of composite materials for structural health monitoring *USACERL Final Technical Paper*
- White S R, Albers R G and Quattrone R F 1996 Tagging of composite materials with Terfenol-D magnetostrictive particles for structural health monitoring *ASME 1996 Mechanics and Materials Summer Meeting (June 1996)* (Baltimore, MD: Johns Hopkins University)
- White S R and Brouwers F 1998 Smart materials for infrastructure applications *Technical Paper, USACERL Contract DACA88-97-K-0001* June 24, 1998
- White S R 1999 Magnetostrictive tagging of composites for health monitoring *Proc. 1999 Int. Composites Expo (Cincinnati, OH, May 1999)* (New York: Composites Institute) pp 22E1–6